DESTABILIZATION OF HOMOGENEOUS BUBBLY FLOW IN AN ANNULAR GAP BUBBLE COLUMN

Fahd M Al-Oufi, Iain W Cumming, Chris D Rielly*

Department of Chemical Engineering, Loughborough University,

Loughborough, Leics, LE11 3TU, UK

ABSTRACT

Experimental results are presented to show that there are very significant differences in the mean gas void fractions measured in an open tube and a annular gap bubble column, when operated at the same gas superficial velocity, using a porous sparger. The mean gas void fraction decreases with increasing ratio of the inner to outer diameter of the annular gap column and the transition to heterogeneous flow occurs at lower gas superficial velocities and lower void fractions. Two reasons are proposed and validated by experimental investigations: (1) the presence of the inner tube causes large bubbles to form near the sparger, which destabilize the homogeneous bubbly flow and reduce the mean void fraction; this was confirmed by deliberately injecting large bubbles into a homogeneous dispersion of smaller bubbles and (2) the shape of the void fraction profiles changes with gap geometry and this affects the distribution parameter in the drift flux model.

KEYWORDS

void fraction profiles, heterogeneous flow, flow transition, two-point conductivity probe

* *Corresponding author email: C.D.Rielly@lboro.ac.uk*

INTRODUCTION

Two-phase gas-liquid flow is an important phenomenon that is harnessed in numerous forms within the chemical and process industries and commonly occurs in a variety of flow geometries such as evaporators, condensers, boilers, fermenters and other gas-liquid reactors. Often these applications involve cases where a gas is bubbled into a liquid and breaks up into a distribution of bubbles sizes, which rise at various velocities towards a free surface; additional processes such as heat and mass transfer and chemical reaction may also occur. Two-phase flow transitions can take place within the equipment as the fraction of gas increases, for example, in steam production (Coulson and Richardson, 1999), or as coalescence and breakage processes alter the bubble size distribution. Typically, two-phase flow behaviour drives the design of related process components: slow chemical process reactions such as oxidation, chlorination, alkylation and many others, which are utilised in the chemical and bio-technological industries, commonly use gas-liquid bubble columns. These columns possess numerous advantages in terms of their simplicity and absence of mechanical moving parts, as well as efficient heat and mass transfer properties, when compared to other types of multiphase reactors (Vijayan *et al*., 2007).

The gas void fraction, α, is an important two-phase flow variable, as it may used to define the occurrence of various flow regimes and is required for the prediction of, for example, the process pressure drop and the heat transfer coefficient; typically the hydrostatic pressure difference, which depends on α, is a significant term in the overall pressure drop. So, two-phase gas-liquid flow is distinguished by being of great utility, yet it is an area of significant difficulty, due to: (i) neither the bubble size nor the gas void fraction are known *a priori* and can vary significantly within a single flow geometry; (ii) a complex array of flow patterns can exist, which are in part determined by the containing flow geometry. In practice, a number of factors, *e.g.* the internal dimensions of the pipe work, physical properties of the gas and liquid phases and flow rates (or superficial velocities) exert considerable influence and determine the flow regime.

In bubble columns with no liquid flow, there are three basic flow regimes: homogeneous, transition and heterogeneous regimes (Deckwer, 1992; Kastanek *et al*., 1993; Molerus, 1993 and Zahradnik *et al*., 1997). These flow regimes are illustrated in Fig. 1 using data obtained in a 0.102 m diameter bubble column (open tube) using air-tap water (Al-Oufi, 2006). The homogeneous regime is characterised by having a uniform dispersion of small spherical or

ellispoidal bubbles and generally occurs at low gas superficial velocities. With increasing gas superficial velocity, the gas void fraction increases and hence the average distance between bubbles is decreased. Hence, at higher gas void fractions, there is an increased probability of coalescence and an increase in bubble size. As the probability of coalescence increases, large bubbles form and this leads to a broad bubble size distribution. Under some circumstances, coalescence leads into the transition regime, where the gas void fraction decreases with increasing gas superficial velocity. At still higher gas superficial velocities the flow comprises large, irregularly shaped bubbles which rise rapidly through a dispersion of smaller ellipsoidal bubbles (in air-water) and α increases once more with increasing j_g in the heterogeneous regime. In Fig. 1, at $j_g \approx 0.12$ m/s, the bubbles reached a maximum concentration at $\alpha = 0.4$ and then start to coalesce; with increasing gas superficial velocity the transition from homogeneous to heterogeneous flow occurs and α falls.

The majority of previous studies of gas void fraction and homogeneous to heterogeneous flow transitions have been for open tube bubble columns of circular cross-section. In the current contribution, annular gap bubble columns are discussed and gas void fraction data are compared with those from open tube bubble columns. These flow geometries commonly occur in the outer annulus of an internal loop air-lift bubble column, formed by concentric tubes; alternatively, the inner tube could be the downcomer and the outer tube could be the riser of a plunging jet bubble column; see, for example, Cumming *et al.,* (2002).

Fig. 1 also shows a comparison of results from an open tube bubble column with data from an annular gap geometry. At the same gas superficial velocities, there is a very significant difference between the measured mean gas void fractions; for the annular gap geometry, the mean value of α can be 50% lower than in the open tube and there is no obvious evidence of a change in flow pattern from homogeneous through transition to heterogeneous flow. The data in Fig. 1 have been fitted according to Zuber and Findlay's (1965) drift-flux model, which has often been used to correlate the gas void fraction across a range of the flow regimes.

$$\alpha = \frac{j_g}{C_0 j_g + v_t} \tag{1}$$

The model contains two adjustable parameters, namely, a velocity, v_t and the distribution coefficient, C_0. Both parameters depend on the radial distributions of gas and liquid velocity and void fraction, as given below

$$C_0 = \frac{\left\langle \alpha \left(j_g + j_l \right) \right\rangle}{\left\langle \alpha \right\rangle \left\langle j_g + j_l \right\rangle} \tag{2}$$

$$v_t = \frac{\left\langle \alpha \, j_{gl} \right\rangle}{\left\langle \alpha \right\rangle} = \frac{\left\langle \alpha \, j_{gl} \right\rangle}{\left\langle \alpha \right\rangle} \tag{3}$$

where j_{gl} is the drift-flux velocity of the gas with respect to the mixture. The parameter v_t is typically close to the single bubble rise velocity and hence depends on the average bubble size in the flow.

Figure 1 shows a least squares fit of the drift-flux model to two experimental data sets for (i) an open tube and (ii) an annular gap bubble column. Typical values for the parameter v_t could fall in the range 0.15 to 0.25 m/s for bubble sizes in the range 3-8 mm; the larger fitted value of v_t for the annular gap column may indicate that larger bubbles were present than in the open tube. The distribution parameters for the two data sets are also significantly different and outside the normally expected range of 0.9 to 1.3 reported by Hibiki and Ishii (2002), which may indicate that the bubble size is increasing with increasing gas superficial velocity. (The values of these fitted parameters are rather sensitive to the exact range of gas superficial velocities used for data regression.) Hasan and Kabir (1992) reported that the distribution parameter did not change with the ratio of inner to outer diameter $\left(\beta = D_i / D_o\right)$ for an annular gap bubble column and remained close to the value of $C_0 = 2.0$ that theyhad previously obtained for large diameters pipes $\left(D_o > 0.1\,\mathrm{m}\right)$. In contrast, Hasan and Kabir (1988a & b) found an increase in β led to a slight increase in C_0, but offered no explanation. The data of Fig. 1 show a much larger effect of the diameter ratio, β, on the distribution parameter. Furthermore, Hasan & Kabir (1992) found that for annular gap bubble columns, v_t remained unchanged from its value in an open tube, which would indicate rather similar bubble sizes in these two cases. Observations of the annular gap column in the current work show that at low j_g, small bubbles were produced; increasing j_g caused these bubbles to merge and form bigger bubbles which destabilized the flow at much lower void fractions and gas superficial velocities than in the open tube bubble column.

For annular channels, several authors (*e.g.* Griffith, 1964; Hasan and Kabir, 1988a & b; Kelessidis and Dukler, 1989; and Hasan and Kabir, 1992) have experimentally verified the theoretical proposal by Radovich and Moissis (1962) that in a vertical pipe, a gas void fraction of about 0.25 triggers the transition from bubbly to slug flow. Fig. 1 shows that clearly this is not a universal statement, as the open-tube results exhibit a homogenous flow regime up to a void fraction of around 0.4, whereas the annular gap flow undergoes a gradual transition to heterogeneous flow at much lower void fractions.

Two reasons are postulated for the differences in gas void fraction between the annular gap and open tube bubble columns: (1) large bubbles form near the sparger, at the bottom of the inner tube in the annular gap system, and these destabilize the flow, such that an earlier flow transition occurs than in the open tube experiments; (2) there are significant differences in the local void fraction and velocity radial profiles, which affect the distribution parameter, C_0 and hence affect the mean gas void fraction. Both of these effects have been studied using a range of annular gap geometries.

EXPERIMENTAL

Open tube and annual gap rig set up

The experimental set-up is illustrated in Fig. 2 and consists of a vertical column of internal diameter (i.d.) $D_o = 0.102\,\text{m}$, made of transparent QVF® glass and with a height of 2.25 m; the unaerated liquid level in the column was 1.00 m. Compressed air was injected through a porous plastic sparger, which covered the whole of the base of the column. In the open tube, the porous sparger had a permeability of $5.3\times10^{-14}\ \text{m}^2$, with a pore size of around 100 μm, and produced a uniform distribution of bubbles; no large bubbles and slugs were observed moving up the open column, at low j_g. The compressed air supply to the base of the column passed through a rotameter connected to a digital pressure gauge; a pressure correction was made to the rotameter reading, which had previously been calibrated at atmospheric pressure.

Annular gap experiments were conducted by using different inner tube diameters, D_i, placed concentrically inside the $D_o = 0.102$ m outer column. Tubes of diameter $D_i = 0.025,\ 0.038,$

0.051 and 0.070 m (o.d.) were used and are denoted by their diameter ratios, $\beta = 0.25, 0.37, .50$ and 0.69 , respectively. These inner columns were sealed and no gas flowed upwards within these tubes; an inverted cone was attached to the bottom of the inner tube and its vertex rested at the centre of the porous sparger. The inner tubes were supported near their top and were aligned to be concentric within the outer column; both columns were carefully aligned to be vertical. The purpose of these experiments was to study the effect of the annular gap geometry on the gas void fraction and on the transition point from homogeneous to heterogeneous flow, in air-water systems (tap water was used in all cases). Prior to the start of all experiments, the air supply was run continuously for about 30 min, to condition the water and hence to obtain reproducible results; other experiments using distilled or RO water gave quite dissimilar results, depending on how long the rig had been operated.

The experiments were conducted in the annular gap columns at the same gas superficial velocities as were used in open tube. The drift flux model, eq.(1), indicates that j_g , equivalent to the gas volume flux, is the key variable in determining the void fraction. The annular gap has a smaller cross-sectional area than the open tube, and so the gas flow rates were adjusted appropriately to cover the same range of j_g .

Overall gas void fractions (volume averages for the whole column) were obtained by recording the volume change on aeration at a given j_g, according to

$$\langle \alpha \rangle = \frac{V_g}{V_g + V_l} \tag{4}$$

In practice, height measurements were used in place of volumes and were conveniently read from a scale on the wall of the column. Local void fractions were also measured using a two-point conductivity probe, as is described in the next section.

Probe design and dimensions

Impedance methods, using one or more electrodes, are popular techniques to measure local void fractions and have been used by many researchers to study different two-phase flow regimes. The electrical conductance of the gas-liquid region surrounding the tips of the electrodes is measured; when the probe tip has penetrated a bubble there is no conductance, whereas when the probe tip is immersed in liquid there is a high conductance. The probe then behaves effectively as a local phase discriminator and the probability (fraction of time)

that the probe is immersed in a bubble is equal to the void fraction. For example, Herringe and Davis (1976) described methods to analyse data from single point conductivity probes for gas-liquid flows; Julia *et al.* (2005) used a single point optical probe to measure local values of α in a gas-liquid flow and showed detailed analysis of how bubbles are pierced (although the detection method is different from conductivity probes the principles of the analysis of very similar); and, Angeli and Hewitt (1999) used this technique to detect flow regimes and measure volume fractions in an oil-water flow. Furthermore, with a two-point probe both the local void fraction and the bubble velocity may be measured; the probe also yields information about the chord length distribution of bubbles intercepted by the probe, from which the true bubble size distributed may be inferred; see for example, Liu and Clark (1995).

Fig. 3 shows a schematic of the conductivity probe which consists of two electrodes and a common earth, which is the outer stainless steel sheath of the probe body. The electrodes are supplied with a high frequency alternating current to prevent electrolysis. The two probes are made from stainless steel needles that are electrically insulated and rendered non-wetting by the application of a varnish, except at the tips which are gold-plated to stabilize the response and to prevent corrosion. Each needle tip was able to pierce, with minimum deformation, the fast-moving small bubbles at the point of impact, leading to a sharp signal response which indicated the passage of a bubble-liquid interface. The probe operated like an electrical switch: when the tip was in contact with the liquid phase—closed circuit—and gas phase—open circuit; Fig. 4(a) shows a typical voltage time history. The tip is the live (+ve) electrode and the outer sheath is the earth in this circuit. The distance between tips has to be adjusted, depending on the bubble sizes and velocities in a two-phase flow system; in these experiments an axial separation of around 5 mm was selected to measure the size and velocity of bubbles with reasonable accuracy. Bubble velocities and sizes will be reported in a later publication and the current contribution concentrates on measurements of the local gas void fraction. The probes were connected to a two channel conductivity meter and the output signals were recorded digitally at 2 kHz using LabVIEW software. The raw voltage measurements were converted in a MATLAB program to give local void fractions using the following algorithm.

1. For any one of the probes (usually probe 1), a histogram of the measured voltages was obtained. Typically this contained two modes: the low voltage mode corresponded the liquid baseline and the high voltage mode corresponded to the gas level.
2. The mean and standard deviation of the liquid baseline was established. Any voltages more than 2 standard deviations above the mean value of the liquid baseline, were taken to be in the gas phase (see fig. 4(a)).
3. The raw data were thus converted to 0 (liquid) or 1 (gas) signals (see fig. 4(b)) and the local gas void fraction was calculated from the time averaged signal.

The distribution of local void fractions was obtained by traversing the probe across the column diameter for the open tube, or radially across the annular gap, at a height of 0.57 m above the sparger. Mean α were obtained by cross-sectionally-averaging the local α profiles (data shown later confirm that these profiles are approximately axisymmetric) according to

$$\overline{\alpha} = \frac{1}{R_o^2 - R_i^2} \int_{R_i}^{R_o} 2r\alpha(r)\, dr \qquad (5)$$

RESULTS AND DISCUSSION

Mean gas void fraction in the annular gap bubble column

A comparison between the gas void fraction in open tube and in different annular gap is illustrated in Fig. 5. Both the volume variation, eq.(4), and conductivity probe methods confirm that the gas void fraction in the open tube is high compared to α values in the annular gap. This is either because large bubbles have been generated in the annular gap, which led to heterogeneous flow, or the radial profile of α profile has changed — the latter would affect the distribution parameter, C_0, in Zuber and Findlay's (1965) drift-flux model. The diameter ratio $\beta = D_i / D_o$ of the annular gap also affects the mean gas void fraction: Fig. 5 shows that when the inner tube size increases, then a lower mean gas void fraction results; there is a significant decrease in the mean α compared to the open tube, confirming the earlier results of Al-Oufi (2006), show in Fig. 1.

Fig. 5 compares data obtained by measuring the changes in aerated level from eq.(4) and from tip 1 of the conductivity probe. The former is a volume-average over the whole column, whereas the latter is averaged across a horizontal cross-section, assuming an axisymmetric

void fraction profile. As stated previously the conductivity probes were located at a height of 0.57 m above the sparger; other heights were also studied (data not shown here), which indicate a small reduction in the void fraction with increasing axial height in the column (due to bubble coalescence), which is one reason for the discrepancy between the data for the two measurement methods in Fig. 5.

Julia *et al.* (2005) discuss how needle probes underestimate the chord lengths of bubbles that are pierced eccentrically from their centre, which would lead to an underestimate of the void fraction. In addition, it is expected that very small bubbles, with diameters less than 1-2 mm may not impact directly on the probe and hence their contribution to the locally measured void fraction may be missing. This is a second reason for why the probe based method underestimates the mean void fraction; the differences between the two types of measurement is around 15%. However, the conductivity probes provide useful information about the void fraction profiles within the column, which cannot be obtained by other measurement techniques.

Destabilization of homogeneous flow by the introduction of large bubbles

The first mechanism by which the mean gas void fraction might be lowered in an annular gap column was investigated, namely that the formation of large bubbles destabilizes the flow and forces an early transition to the heterogeneous regime. Larger bubbles were deliberately introduced into the flow through a single orifice drilled in the centre of the porous sparger. The open tube column was used for this set of experiments and various orifice diameters were investigated from 0.4 to 3.0 mm; each generated a stream of large bubbles, which rose rapidly through the dispersion of more uniformly sized bubbles produced by the surrounding porous plate sparger. Fig. 6 (a) and (b) represent the results obtained from the volume change and conductivity probe methods respectively; for the latter, mean gas void fractions were obtained by volume-averaging the local α distributions, using eq.(5). As noted previously, Fig. 6, shows that the conductivity probe mean gas void fractions agree fairly well with the volume variation results and certainly qualitatively consistent behaviour is observed using both measurement methods. For the open tube bubble column, it was observed that at low j_g, small and uniform bubbles in homogeneous flow were generated by the porous plastic sparger which had no orifice.

When the porous plastic sparger was drilled with small orifice diameters < 1mm, there was very little effect on the mean gas void fraction, as shown in Fig. 6 (a). The bubbles produced from these small orifices were not sufficiently different from those produced by the porous sparger and hence there was no effect on the flow stability or mean void fraction. For perforated plate spargers, the literature (*e.g.* Zuber and Hench, 1962) suggests that the orifice size has to be greater than 1 mm to generate heterogeneous flow at all j_g. In Fig. 6 (a) and (b) the effect of large bubble generation from the orifice starts to take place at a diameter of 2 mm; these bubbles rise much faster than the smaller spherical bubbles produced by the porous plate; with increasing gas superficial velocity, an increasing fraction of the gas flow is transported as large bubbles and consequently the measured gas void fraction is reduced compared to the normal porous sparger. The results in Fig. 6 show that the large orifice diameters (> 2mm) generates large bubbles which destabilize the homogeneous flow; the transition to heterogeneous flow occurs at a lower void fraction, with increasing orifice size. At the largest orifice size, it is difficult to detect exactly when the transition occurs and for the whole range of j_g the flow regime appears to be heterogeneous, with both large and small bubbles present.

Zuber and Hench (1962) carried out experiments over the same range of gas flow rates using a variety of perforated plates as air dispersers; see table 1. From their experiments, as the hole size in the gas distributor plate was decreased (number of orifices was increased), higher gas void fractions were generated; an initially homogeneous regime was obtained at low superficial velocities, when the hole size was 0.41 mm, as is shown in Fig. 7; larger orifices gave heterogeneous flow over a much wider range of gas superficial velocities. So the orifice diameter plays a role in determining the gas void fraction, by destabilization of the homogeneous regime. The present results are compared with those by Zuber and Hench (162) in Fig. 7. There is good agreement for the porous sparger (without central orifice) with Zuber and Hench's (1962) results for their perforated plate with 0.41 mm diameter holes (289 orifices). The magnitude of the reduction in the mean gas with increasing orifice size is greater in Zuber and Hench's results, but the effects are qualitatively similar: larger orifice sizes generate large bubbles, which sweep the smaller bubbles into their wake, causing coalescence and hence an early transition to the heterogeneous regime occurs.

Local gas void fraction profiles

The advantage of the conductivity probe methods is that they are able to determine *local* gas void fractions and by traversing the probe, α profiles can be measured. Fig. 8 shows the α profile obtained by traversing the probe across a diameter of the open tube bubble column at a height of 0.57 m above the sparger; because of the radius of the bend in the probe body, it is not possible to measure very close to the near wall of the column, whereas it is possible to access within 5 mm of the far wall.

The profiles are axisymmetric about the line $y = 0.052$ m on the centre-line of the bubble column, justifying the use of eq.(5) to calculate the mean α. At low j_g the results show almost uniform distributions of the local void fraction across the column; in the homogeneous flow regime (j_g < 0.1 m/s), the void fraction profiles become increasingly non-uniform with increasing gas superficial velocity: the ratio of the centreline void fraction, α_c, to the wall void fraction, α_w, increases significantly. Hibiki and Ishii (2002) fitted their void fraction profiles with a power-law equation

$$\frac{\alpha - \alpha_w}{\alpha_c - \alpha_w} = 1 - \left(\frac{r}{R_o} \right)^n \tag{6}$$

Here the exponent n defines the shape of the non-dimensionalised profile. Hibiki and Ishii (2002) show that n affects the value of the distribution parameter in the drift-flux model, eq.(1). It is clear from Fig. 8 that n would be an increasing function of gas superficial velocity in the homogeneous regime. In contrast, in the transition and early parts of the heterogeneous regime (j_g > 0.1 m/s), the void fraction profiles approximately collapse onto a single curve, for which n would remain almost fixed. Under these conditions, the majority of the bubbles tend to travel in the centre of the column and fewer bubbles travel close to the wall; coalescence is more likely to occur close to the centre-line of the column, giving large, fast-rising bubbles, surrounded by small bubbles at the wall, in the transition and heterogeneous flow regimes.

Fig. 9 shows the radial void fraction profiles for the four annular gap geometries that were studied; the centreline of the annular gap at $r = (R_i + R_o)/2$ is also marked for reference. Similar trends are observed compared to the open tube bubble column. At low gas superficial velocities, the void fraction profiles are almost flat, but grow increasingly non-uniform with

increasing j_g. At the higher gas superficial velocities, the profile shape becomes almost constant and independent of j_g. Unlike the open tube, the α profiles in the annular gap are not symmetric about the centreline; the maximum of the profile is displaced towards the inner wall. With increasing diameter ratio, $\beta = D_i / D_o$, the maximum moves closer to the inner wall of the annular gap and the maximum gas holdup increases. Ozar *et al*. (2008) measured and correlated void fraction profiles in annular gaps, albeit over very different ranges of gas and liquid superficial velocities to those studied here. They proposed power-law equations to represent the void fraction profiles according to

$$\frac{\alpha}{\langle \alpha \rangle} = \frac{n}{n+1}\left(1 - \left|1 - \frac{2(r - R_i)}{R_o - R_i}\right|^n\right) \tag{7}$$

and showed that the distribution parameter C_0 was related to the exponent n. The effect of increasing n in eq.(7) is to flatten the void fraction profile, but it remains symmetric about the centreline of the channel, which was approximately true for Ozar *et al.*'s (2008) data. Thus, the data of Fig. 9 cannot be successfully correlated by an expression of the form of eq.(7) and clearly the shape of the profile changes with the geometry of the annular gap. Gas velocity profiles are available from the two-point conductivity probe (to be reported elsewhere), but liquid velocity profiles were not available and hence eqs.(2) and (3) could not be directly applied to calculate the C_0 distribution parameters for each case. Nevertheless the results of Fig. 9 indicate that C_0, which is a measure of non-uniformity in the column, is likely to increase above unity, with increasing diameter ratio β (as was shown in Fig. 1). In that case, eq.(1) indicates that the mean void fraction should decrease with increasing β, for a given gas superficial velocity, *i.e.* the mean gas hold falls with increasing diameter of the inner column, which is what has been observed experimentally in Fig. 5.

CONCLUSIONS

Two main effects have been considered in this study, which reduce the mean void fraction in annular gap columns compared to empty bubble columns, when operated at the same gas superficial velocity and with a porous sparger. Firstly, the introduction of a stream of larger bubbles emanating from a central orifice drilled into the porous sparger has been shown to destabilization an otherwise homogeneous bubbly flow; orifices with diameters greater than

1-2 mm, produced fast rising bubbles and the transition to heterogeneous flow occurred at lower mean gas void fractions than for the porous sparer with no central orifice; in some cases the flow appeared to be heterogeneous even at very low gas superficial velocities. In annular gap columns, large bubbles are observed in the flow, even at relatively low gas superficial velocities. Similar results for the effects of sparger design on the two-phase flow regime can be found in the literature, for example in the work of Zuber and Hench (1962). Secondly the local void fraction profiles changed shape with increasing gas superficial velocity in the homogenous regime, indicating that for open tube columns the distribution parameter, C_0 may not be constant. For the annular gap columns, the shapes of the local void fraction profiles are affected by the diameter ratio, $\beta = D_i / D_o$; as β increases the void fraction profiles become increasingly non-uniform and asymmetric and hence the value of C_0 is expected to increase, leading to a reduction in the mean gas holdup predicted by the drift flux model. Thus the combination of large bubble formation near the sparger and changing shapes of the *local* gas void fraction profile, reduce the mean gas void fraction for a given gas superficial velocity, and lead to an earlier transition to heterogeneous flow than would occur in an open tube bubble column.

NOMENCLATURE

C_0	distribution parameter used in eq.(1) for the drift flux model (–)
D_i	diameter of the inside column (m)
D_o	diameter of the outside column (m)
j_g	gas superficial velocity (m/s)
j_{gl}	drift flux velocity (m/s)
j_l	liquid superficial velocity (m/s)
R_i	radius of the inside column (m)
R_o	radius of the outside column (m)
V_g	volume of gas (m^3)
V_l	volume of liquid (m^3)
v_t	single bubble rise velocity used in eq.(1) for the drift flux model (m/s)

Greek

α	gas void fraction (–)

β diameter ratio D_i / D_o of the annular gap column (–)

REFERENCES

Al-Oufi, F.M., "Measuring void fractions in gas-liquid flows using conductivity rings", MSc report, Department of Chemical Engineering, Loughborough University, UK, (2006).

Angeli, P. and G.F. Hewitt, "Flow structure in horizontal oil–water flow", Int. J. Multiphase Flow, **26**(7), pp.1117-1140 (1999)

Coulson, J.M., J.F. Richardson, J.R. Backhurst, and J.H. Harker, "Coulson & Richardson's Chemical Engineering", Volume 1, Butterworth-Heinemann, Boston MA, (1999), pp.149-195.

Cumming, I.W., C.D. Rielly, and A.J. Mason, "Hydraulic performance of an annular plunging jet factor", Trans. I. Chem. E., Part A, **80,** pp. 543-549, (2002).

Deckwer, W., "Bubble column reactors", Wiley (1992), pp. 159-168.

Griffith, P., "The prediction of low quality cooling voids" J. Heat Transfer, pp. 327-333, (1964).

Hasan, A.R. and C.S. Kabir, "A study of multiphase flow behaviour in vertical oil wells", SPE Prod. Eng., **3**, pp. 263-272, (1988a).

Hasan, A.R. and C.S. Kabir, "Predicting multiphase flow behaviour in a deviated well" SPE Prod. Eng., **3**, pp. 474-482, (1988b).

Hasan, A.R. and C.S. Kabir, "Two-phase flow in vertical and inclined annuli", Int. J. Multiphase Flow, **18**(2), pp. 279-293, (1992).

Herringe R.A. and M.R. Davis, "Structural development of gas–liquid mixture flows", J. Fluid Mech. **73**(1), pp. 97–123, (1976).

Hibiki, T. and M. Ishii, "Distribution parameter and drift velocity of drift flux model in bubbly flow", Int. J. Multiphase Flow, **45**, pp. 707-721, (2002).

Julia, J., W. Harteveld, R. Mudde, and H.E.A.van den Akker, "On the accuracy of the gas void fraction measurements using optical probes in bubbly flows", Rev. Sci. Instruments, **76**(3), pp. 035103-1 – 035103-13, (2005)

Kastanek, F., J. Zahradnik, J. Kratochvil, and J. Cermak, “Chemical reactors for gas-liquid systems”, Academia Praha, [Ellis Horwood] (Prague, [New York]), (1993), Ch. 3.

Kelessidis, V.C. and A.E. Dukler,. “Modelling flow pattern transitions for upward gas-liquid flow in vertical concentric and eccentric annuli” Int. J. Multiphase Flow, **15**(2), pp.173-191, (1989)

Liu, W. and N.N. Clark, “Relationships between distributions of chord lengths and distributions of bubble sizes including their statistical parameters”, Int. J. Multiphase Flow 1995 (6), pp. 1073-1089, (1995).

Molerus, O., “Principles of flow in disperse systems”. London: Chapman & Hall, (1993).

Ozar, B. J.J. Jeong, A. Dixit, J.E. Juliá, T. Hibiki, M. Ishii, “Flow structure of gas--liquid two-phase flow in an annulus”, Chem. Eng. Sci. **63**, pp. 3998 - 4011, (2008)

Radovich, N.A. and R. Moissis, “The transition from two phase flow to slug flow” Report No. 7-7673-22, Dept of Mech. Eng., MIT, Cambridge, MA (1962).

Vijayan, M., H.I. Schlaberg, H.I. and M. Wang, “Effects of sparger geometry on the mechanism of flow pattern transition in a bubble column” Chem. Eng. J., **130**(2-3), pp. 171-178, (2007).

Zahradník, J., M. Fialová, M. Ruzicka, J. Drahos, F. Kastaek, F. and N.H. Thomas, “Duality of the gas-liquid flow regimes in bubble column reactors”, Chem. Eng. Sci, **52**(21-22), pp. 3811-3826, (1997).

Zuber, N. and J.A. Findlay, “Average volumetric concentration in two-phase flow system”, J. Heat Transfer, **87**, pp. 453-468 (1965).

Zuber, H. and J. Hench, “Steady state and transient gas void fractions of bubbling systems and their operating limits” General Electric Company, Report No. 62GL 100, (1962).

Table 1 Gas distributor configurations used by Zuber and Hench (1962)

No. of orifices	Diameter (mm)	Square array spacing (mm)
1	4.06	-
49	4.06	6.25
100	1.52	9.5
289	0.41	6.25

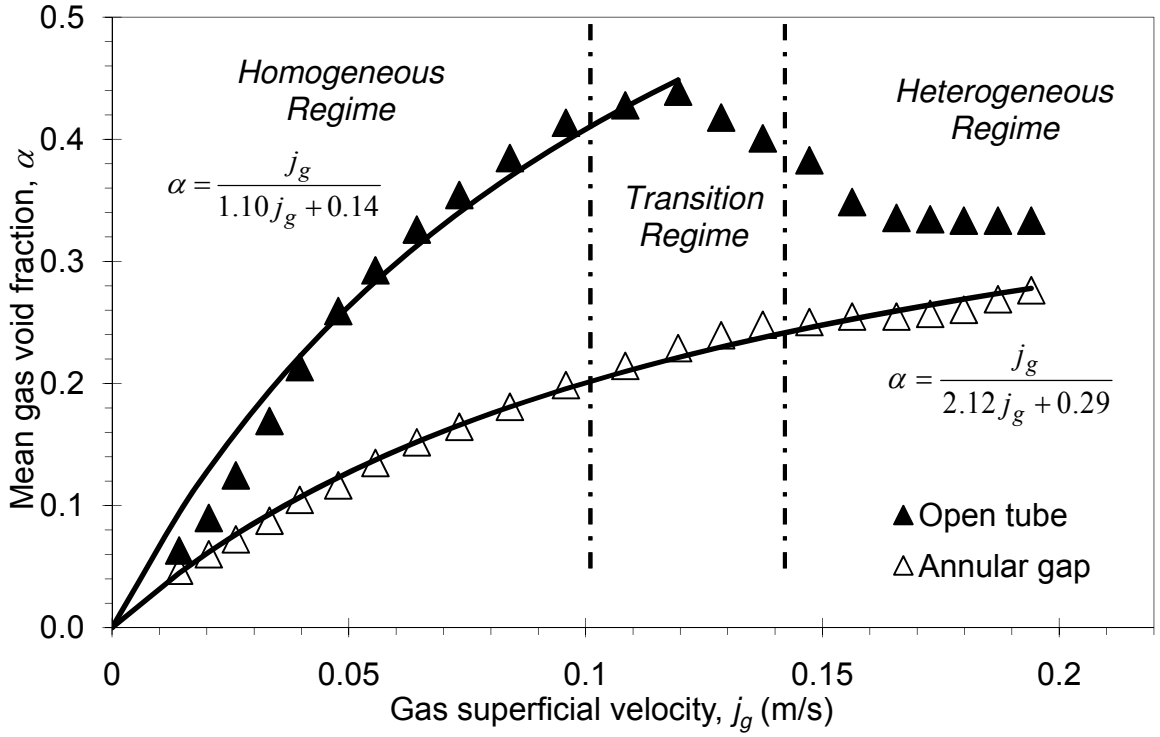

Fig. 1 Comparisons of measured gas void fractions for air – tap water in (i) an open tube (D_o = 0.102 m) and (ii) an annular gap bubble column ($D_i = 0.051\,\text{m}$, $D_o = 0.102\,\text{m}$). The mean gas void fraction was obtained from the change of level in the bubble columns on aeration; data from Al-Oufi (2006).

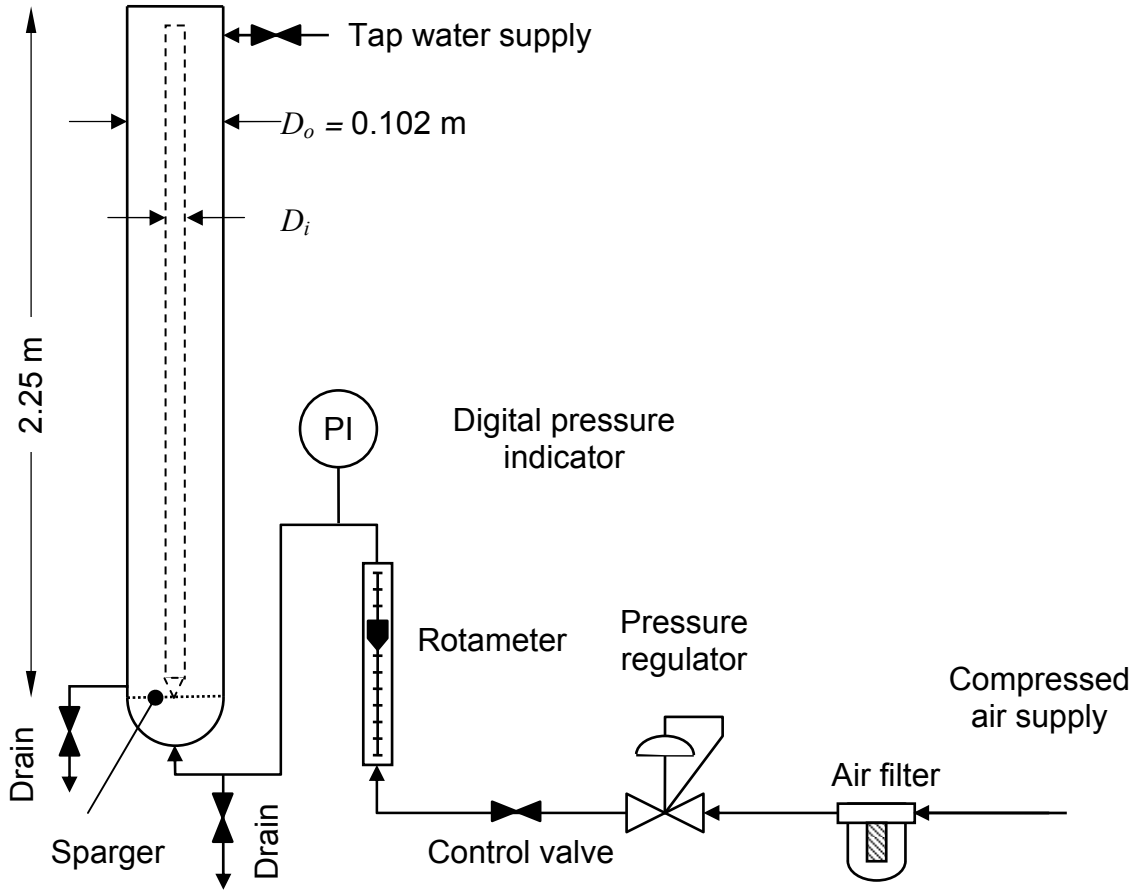

Fig. 2 The experimental set up for the open tube and annular gap bubble columns.

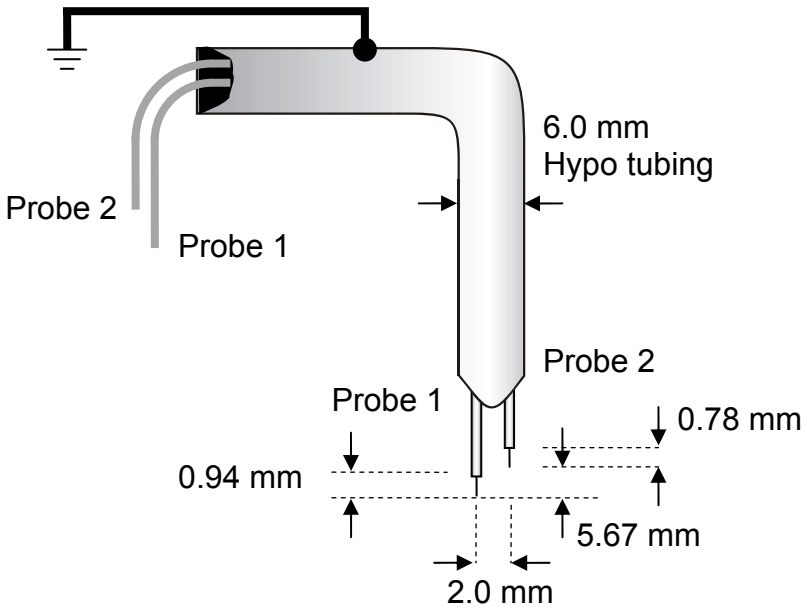

Fig. 3 Design and geometry of the two-point conductivity probe (not to scale).

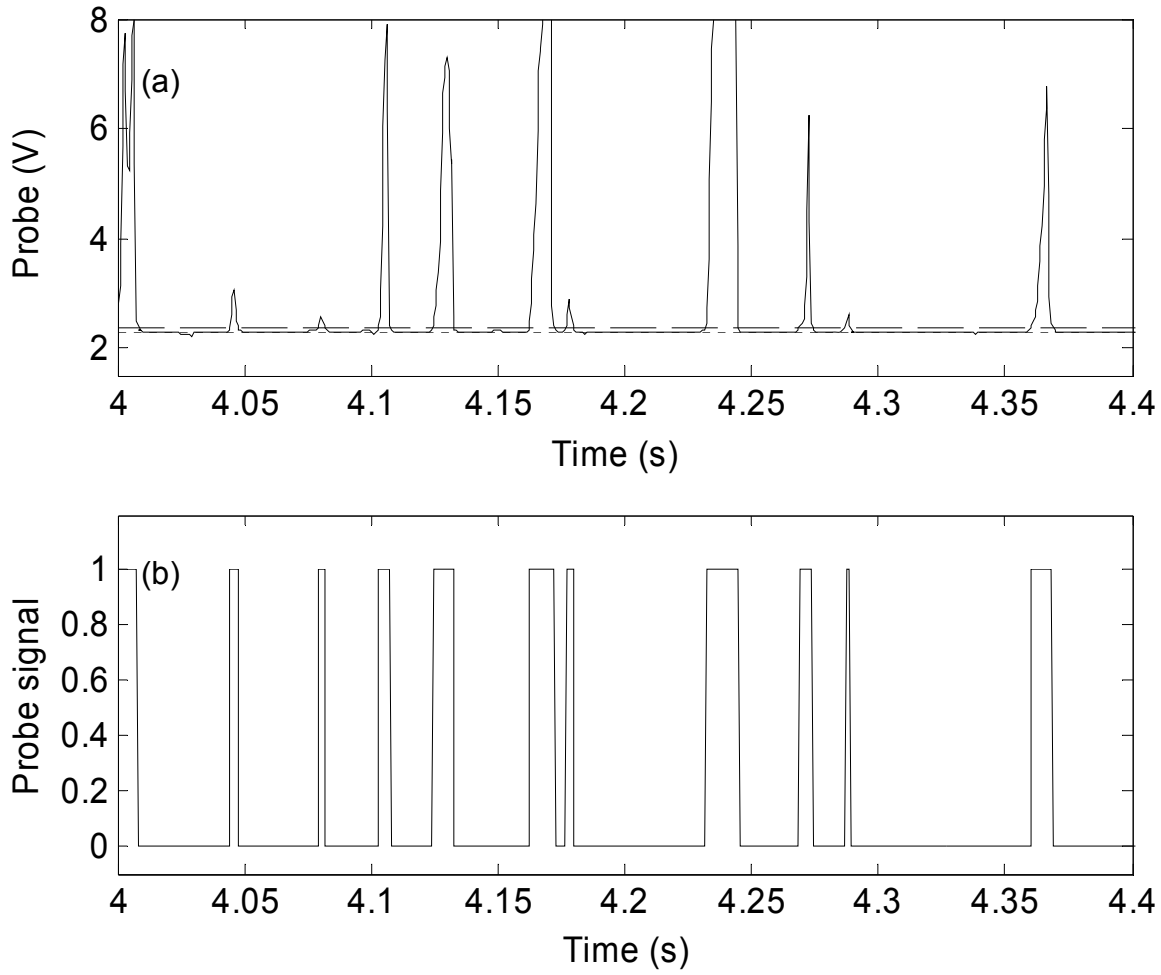

Fig. 4 Signals obtained from a single conductivity probe: (a) raw data, showing lower liquid base-line and 2 standard deviations above the mean and (b) the phase discriminated data, where 0 is the liquid phase and 1 is the gas phase.

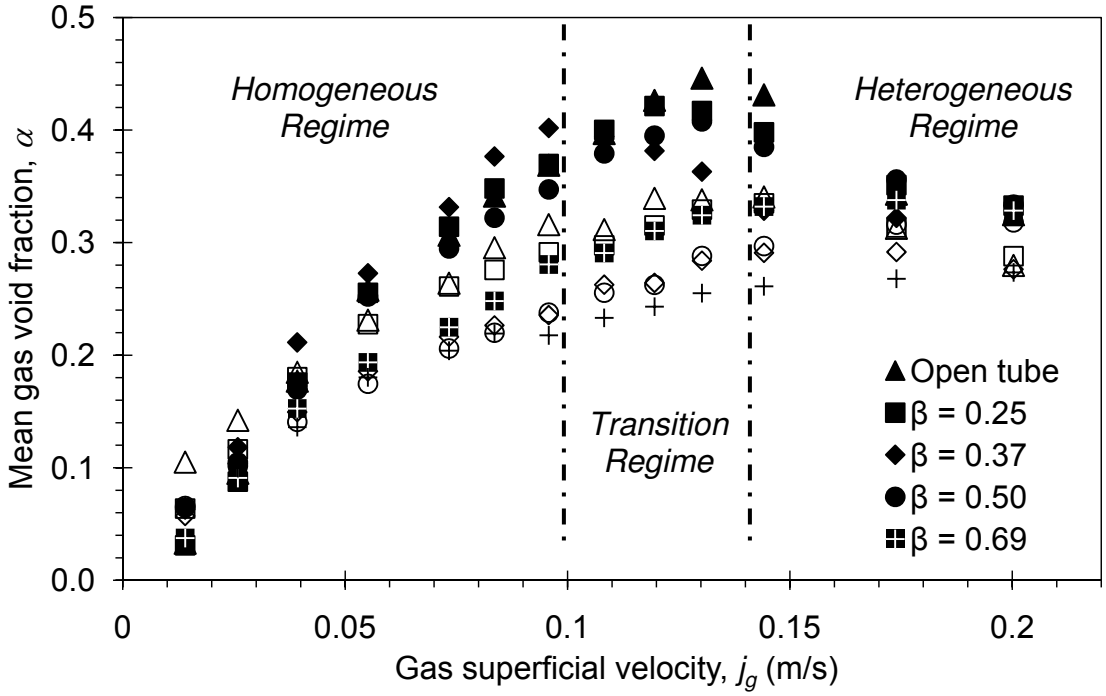

Fig. 5 Mean gas void fraction in the annular gap columns compared to the open tube results; closed symbols from measurements of the change of aerated height, eq.(4), and open symbols from measurements using the conductivity probe.

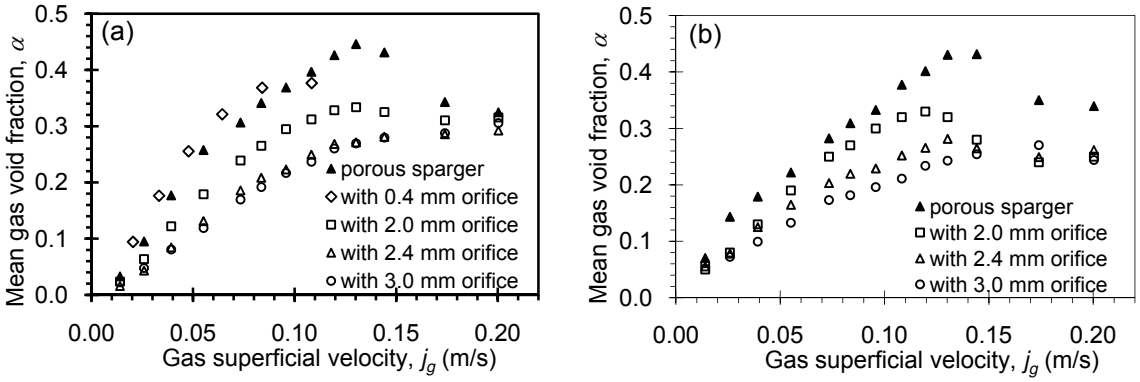

Fig. 6 Mean void fraction variations with superficial gas velocity for the porous sparger, with and without various diameters of single orifice: (a) volume mean obtained by change in aerated height and (b) cross-sectional mean determined by the conductivity probe method (probe 1).

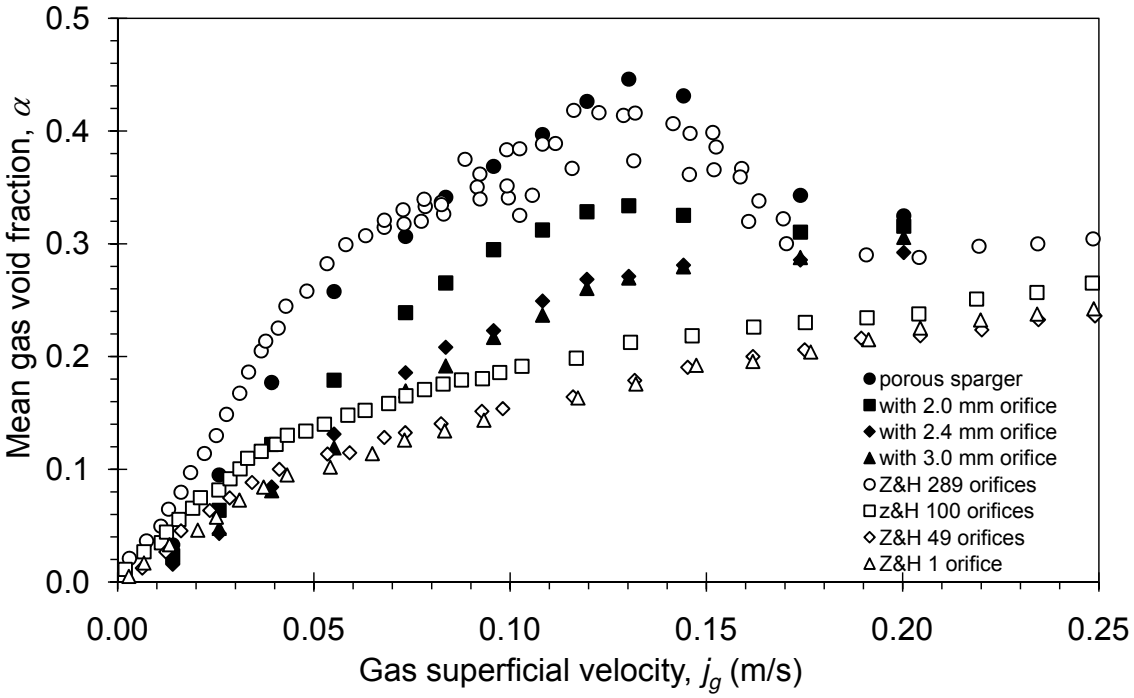

Fig. 7 Mean gas void fractions for the normal porous sparger and for the same sparger with different central orifice hole sizes; comparisons with Zuber and Hench's (1962) results (see table 1 for details of their perforated plate spargers).

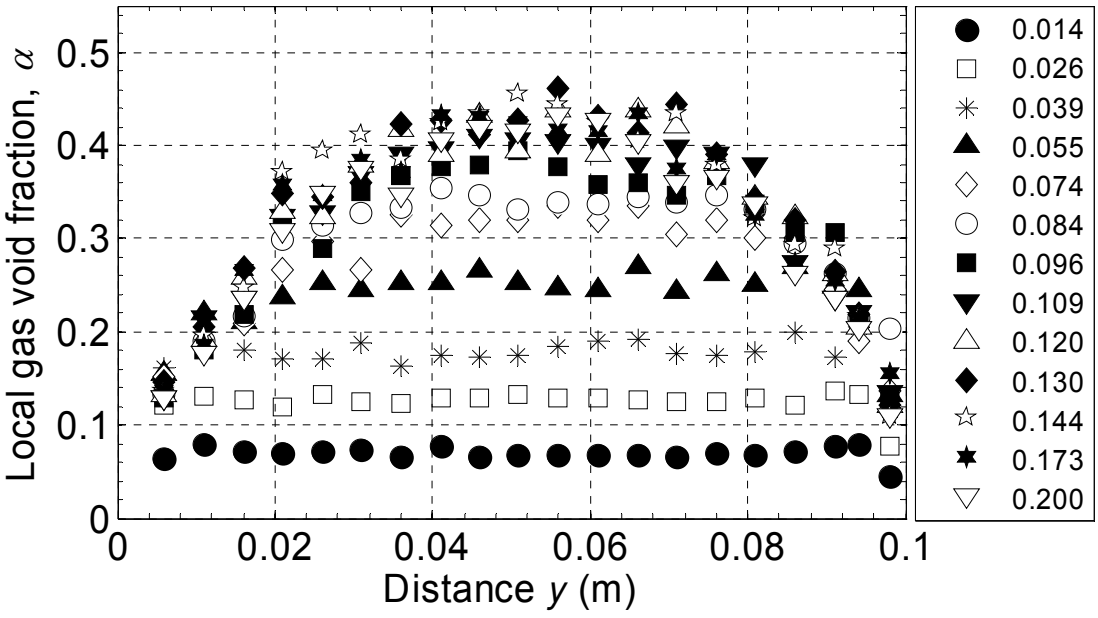

Fig. 8 Profiles of the local gas void fraction with distance from the wall, *y,* across a diameter of the open bubble column, with the porous sparger. The legend gives the gas superficial velocity (m/s).

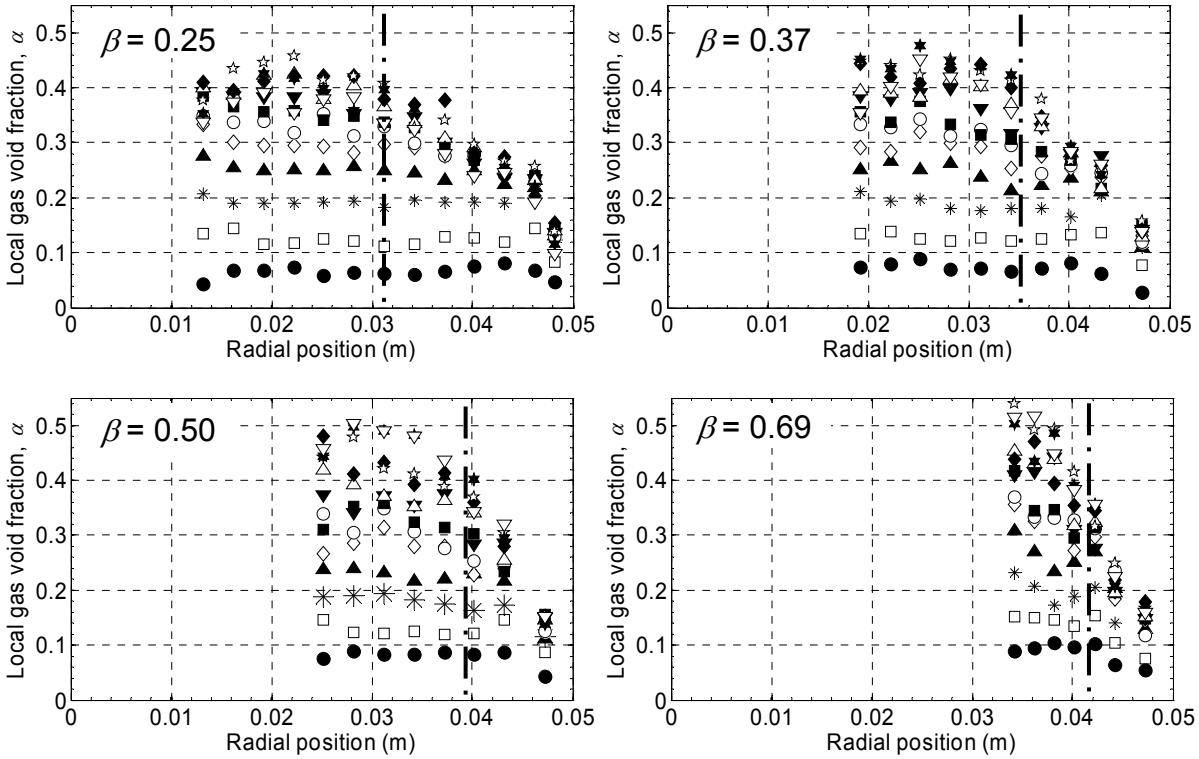

Fig. 9 Radial profiles of the local gas void fraction for different geometries of the annular gap bubble column, with the porous sparger. The vertical dashed lines indicate the centreline of the annulus and legend is the same as in fig. 8.